Implementation of an intensity interferometry system on the StarBase observatory

Nolan Matthews, Orville Clarke, Shaun Snow, Stephan LeBohec, David Kieda

Nolan Matthews, Orville Clarke, Shaun Snow, Stephan LeBohec, David Kieda, "Implementation of an intensity interferometry system on the StarBase observatory
," Proc. SPIE 10701, Optical and Infrared Interferometry and Imaging VI, 107010W (9 July 2018); doi: 10.1117/12.2312716

SPIE.

Event: SPIE Astronomical Telescopes + Instrumentation, 2018, Austin, Texas, United States

Implementation of an intensity interferometry system on the StarBase observatory

Nolan Matthews[a], Orville Clarke[a], Shaun Snow[a], Stephan LeBohec[a], and David Kieda[a]

[a]University of Utah, 115 S 1400 E, Salt Lake City, USA

ABSTRACT

A modern implementation of a stellar intensity interferometry (SII) system on an array of large optical telescopes would be a highly valuable complement to the current generation of optical amplitude interferometers. The SII technique allows for observations at short optical wavelengths (U/B/V bands) with potentially dense (u,v) plane coverage. We describe a complete SII system that is used to measure the spatial coherence of a laboratory source which exhibits signal to noise ratios comparable to actual stellar sources. A novel analysis method, based on the correlation measurements between orthogonal polarization states, was developed to remove unwanted effects of spurious correlations. Our system is currently being tested in night sky observations at the StarBase Observatory (Grantsville, Utah) and will soon be ported to the VERITAS (Amado, AZ) telescopes. The system can readily be integrated with current optical telescopes at minimal cost. The work here serves as a technological pathfinder for implementing SII on the future Cherenkov Telescope Array.

Keywords: Intensity Interferometry, IACT, StarBase, VERITAS, CTA, High-resolution astronomical imaging

1. INTRODUCTION

Intensity Interferometry (II), as applied to astronomical sources, has undergone a resurgence of interest in the past decade due to the possibility of performing interferometric observations at large baselines ($> 500\,\mathrm{m}$) with wide wavelength coverage (ultra-violet to infrared) and polarimetry capability. Such observations would complement the current generation of optical interferometric observatories that operate at relatively shorter baselines in the visible and infrared. The II technique was abandoned in the 1970's after the completion of the very successful and pioneering observing program of the Narrabri Stellar Intensity Interferometer[1] (NSII) due to poor sensitivity when compared to the then emerging techniques in amplitude interferometry. However, thanks to advances in detector light collection efficiency and high-speed digital electronics, as well as the construction of large optical telescope arrays, a modern II observatory can be designed and constructed to achieve sensitivities operating at the blue end of the visible spectrum ($\lambda < 450\,\mathrm{nm}$) over unprecedented baselines. The NSII was limited to very bright stars[2] with apparent visual magnitude $m_v < 2.5$ but recent studies highlight the possibility of obtaining stellar diameter measurements for sources with $m_v < 6$ in a single night of observation using current observatories and off-the-shelf instrumentation.[3]

Consequently, several efforts have recently been made towards the development of a modern II observatory. Notably, there has been the successful II measurement of the coherence of bright stars with a single 1 m telescope using single photon counting detectors.[4] There are ongoing II measurements with the Aquaeye+ and Iqueye instruments in Asiago[5] which also utilize single photon counting detectors. By spectrally filtering the light through extremely narrow-band filters it has been possible to resolve the temporal coherence of sunlight;[6] This was observed through variable weather conditions without significant degradation of the signal.[7] Such work into temporal intensity interferometry has potential application in characterizing narrow emission lines from astrophysical sources.[8] The potential of a multi-channel intensity interferometer[9] also allows for increased sensitivity and/or increased wavelength coverage. Linear polarization filters can be used to allow for polarization resolved measurements, and also allow for the removal of systematic noise due to spurious correlations.[10]

Further author information: (Send correspondence to N.M.)
N.M.: E-mail: nolankmatthews@gmail.com
D.K.: E-mail: dave.kieda@physics.utah.edu

Optical and Infrared Interferometry and Imaging VI, edited by Michelle J. Creech-Eakman, Peter G. Tuthill, Antoine Mérand, Proc. of SPIE Vol. 10701, 107010W · © 2018 SPIE
CCC code: 0277-786X/18/$18 · doi: 10.1117/12.2312716

(a) (b)

Figure 1: LEFT: Photograph of one of the StarBase reflectors. Each telescope consists of 19 individual hexagonal mirror facets resulting in a total diameter of 3 m. The light from the mirrors is directed towards the SII camera consisting of a single PMT or 'pixel'. RIGHT: Photograph of the StarBase camera. Light is directed onto an optical interface (described in text) and detected by the PMT.

It has been long foreseen that Imaging Air-Cherenkov Telescope (IACT) arrays could be used for II measurements by taking advantage of the large light collection areas and nanosecond time resolution capabilities needed for gamma-ray induced air shower observations.[11] Furthermore, II measurements can take place during bright moonlight conditions[12] when gamma-ray observations are marginally feasible. A tantalizing opportunity is to outfit the future Cherenkov Telescope Array[13,14] (CTA) with II capabilities. For the approximate 100 telescopes planned for the southern CTA observatory site, an unprecedented number of almost 5000 simultaneous baselines would be available over kilometer distance scales. With such dense (u,v) plane coverage, direct image reconstruction becomes possible.[15,16] A study using the CTA observatory highlights numerous science targets for observation.[17]

Although it is attractive to instrument IACT observatories with SII capabilities, there are significant challenges in doing so. Principally, most IACT telescopes are constructed with fast focal ratios (typically f/1 to f/1.4) which complicates the use of interferometric narrow-band filters that require collimated light. Dedicated hardware is needed in order to record each individual data stream either to disk for post-processing, or have them communicated to a real-time correlator. The data from different telescopes must be synchronized at nanosecond timescales across kilometer baselines. The correlator has to be able to process the extremely large volumes of data. This manuscript presents several solutions to these issues as identified during laboratory measurements and ongoing tests with the StarBase observatory.

2. THE STARBASE OBSERVATORY

The testbed observatory StarBase was constructed to test and validate a working II system for a telescope design comparable to what is used in IACT arrays. It is located in Grantsville, Utah, at a latitude of 40.648^o N, a longitude of 112.525^o W and an elevation of 1311 m.a.s.l. It consists of a pair of identical 3 m diameter telescopes, separated by a distance of about 21 m with a 94.3^o azimuth angle with respect to a North-South baseline. The telescopes are constructed in the Davies-Cotton optical design with an f/1 focal ratio, typical of telescopes used in IACT arrays. The reflectivity of the mirrors is approximately 85% over the wavelength range of 370 - 450 nm. Tracking is performed via a LabVIEW software program. A CCD camera mounted onto one

of the beams of the telescope is used to view the position of the star image in the focal plane. Corrections in the altitude and azimuth can then be applied in order to slew the star image into and out of the II optics. The physical point-spread function (PSF) in the focal plane is approximately 1.3 cm, corresponding to an angular PSF of 0.2^o. For II observations, this PSF is the main factor for the limiting observable stellar magnitude due to the contribution of night sky background (NSB) photons. For a nominal NSB light level of 21.5 mag/arcsec^2 in the B photometric band,[18] the limiting stellar magnitude must be less than 4.7 for the NSB not to exceed 50% of the expected photon flux from the target star. An initial implementation of an II system using analog electronics was deployed onto the StarBase telescopes[19] but was abandoned due to unconstrained electronic noise issues and replaced with a high-speed digital system using FPGA based data processing. The digitizing system allows for careful examination of systematics, real-time computation of the correlation, and can be scaled to a large number of additional telescopes.

2.1 Optical System

The starlight focused by the spherical mirror facets is redirected by a mirror making a 45^o angle with the optical axis and is mounted a few centimeters before the focus. Other optical elements are mounted onto an optical breadboard. At the focus, a 1.3 cm optical diaphragm matching the physical PSF of the telescope selects star light, reduces stray light, and is used for tracking monitoring. The starlight then goes through a linear polarization filter. On one of the telescopes the polarization is fixed. On the other, the polarization is switched to be parallel or orthogonal with respect to the fixed polarization telescope. The polarization modulation is introduced to allow for background correlation measurements, which are used in order to subtract undesired spurious correlations. The light then goes through an interferometric narrow-band filter with a center wavelength of $\lambda = 420$ nm and a specified bandwidth of $\Delta\lambda = 5$ nm. Generally, interferometric optical filters require that the light be collimated and the performance is severely degraded in the f/1 optics of the StarBase telescopes. However, we chose a filter with coating with a high refractive index ($n = 2.38$) in order to minimize the effect of non-normal incident rays. Simulations indicate an effective bandwidth of $\Delta\lambda \approx 10$ nm centered at $\lambda = 416$ nm. Finally, a single high quantum-efficiency ($> 30\%$) Hamamatsu R10560 photomultiplier tube (PMT) collects the light.[20] The total throughput of the system using estimates of the transmission of the mirrors, individual filters, and detector quantum efficiency is estimated to be 10% and is in fair agreement with the measured photon rates.

A notable feature of this design when considering an implementation onto IACT telescope cameras is the low physical profile of the optical hardware needed on the camera for II observations. For operation using a single PMT, only three optical elements (collimating lens, polarizing and narrow-band filter) are needed. In the current setup, the polarization is modulated via the use of a sliding filter. When the design is ported onto a IACT camera it could be more convenient to use a motorized rotating mount for the polarization filter to reduce the physical dimension, and reduce systematics associated with multiple filters. Another alternative to polarization modulation is to use a broadband light source in which the temporal coherence is negligible.[4]

2.2 Data acquisition and correlator hardware

The current from each PMT is conditioned by a low-noise high-speed transimpedance preamplifier. RG223 Pasternack double shielded coax cables take the signal from each PMT to a central processing system based on National Instruments (NI) hardware. The voltage signal is digitized by an NI-5761 250 MS/s 14-bit AC-coupled analog-to-digital converter (ADC). An anti-aliasing filter of electronic bandwidth $\Delta f = 125$ MHz is inserted before the ADC in order to improve noise rejection as well as satisfy Nyquist sampling. After digitization, an NI-7965R FPGA module which hosts a Virtex-5 FPGA chip is then used to perform further digital signal processing. The FPGA is programmed using LabVIEW software so it can be used to either perform the real-time cross-correlation at the time of observation, or stream the data continuously to disk for post-acquisition correlation analysis. In order to allow for a large range of photon rates, the FPGA correlator developed for StarBase can operate in two modes. In the 'linear mode', data is recorded as a digitized voltage. In the 'photon counting mode', individual photons are identified by thresholding. In the case where the photon rate is on order or greater than the sampling rate, it becomes impossible to record individual photons, and the linear mode is then chosen. When the photon rate is much less than the sampling rate, individual photons can be discriminated, and it is advantageous to use the photon counting mode to reduce systematics. The current implementation of the FPGA correlator is based on a multiply-accumulate algorithm. It can process the correlation at the digitization rate

(250 MHz). For StarBase, where only two telescopes are used this is more than adequate. However, for an array of II telescopes, greater processing capabilities would be needed. In that case, since correlation measurements can easily be parallelized, multiple FPGAs could be employed to reduce the computation time.

2.3 Data synchronization

The digitization of the signals recorded at each telescope must be phase-locked to within the sampling frequency corresponding to the electronic bandwidth of the system. If phase synchronization is lost, the coherence signal will be effectively smeared across multiple samples, degrading the achievable SNR. In StarBase, the baseline of 21 m is small enough to allow the use of identical length cables to bring both signals to a single ADC module in-phase. However, for much larger baselines ($>$ 100m), like those envisioned within CTA, it is more realistic to have the digitization modules physically close to each telescope. In this case, a central timing system must be used to phase-lock the separated ADC modules. This has already been tested in our setup by the use of a White Rabbit (WR-LEN) timing module. The module consists of a central master clock which distributes a 10 MHz signal via optical fiber to remote receiver modules. The distributed signals are specified to be phase-locked to a fraction of a nanosecond, adequate for sampling rates up to about 1 GHz. In our current system, the digitizer is phase-locked to the 10 MHz signal via the use of NI-6674T timing modules. This module, which is connected to the same backplane chassis as the digitizer, generates a backplane clock based on the input signal, from which the digitizer clock is referenced. In the laboratory we have demonstrated II measurements under conditions comparable to that of star-light measurements using separated chassis.

2.4 Observations

To begin tracking, both telescopes are slewed to the star of interest and any necessary tracking corrections are applied in order to center the star onto the II optics. Initially, this is visually verified using the CCD camera image. Once the high voltage (HV) for the PMT is applied, the pointing can be better improved by maximizing the observable PMT photon rates via further tracking corrections. Periodically, the telescopes are slewed off source to measure the level of the NSB, and PMT dark count rate. The PMT background rate is generally found to be less than 5% of the signal rate associated with the star for sources with $m_B < 2.0$.

The current system at StarBase utilizes the FPGA to perform real-time correlations. Due to the relatively small mirror area, the photon rates recorded for stars of interest is generally much less than the sampling rate, thus prompting the photon counting mode. The correlogram, or cross-correlation over -128 to 128 ns in steps of 4 ns, is recorded to disk every 1 s. Each of these accumulations are stored concurrently with the total photon count over the accumulation period for both channels, GPS timestamp, and the run-tag (ie. ON or OFF). The run-tag refers to the polarization between telescopes being parallel (ON) or orthogonal (OFF). Each ON or OFF run is typically 10 minutes in duration, and alternate evenly throughout the observation. A Python script integrates the stored correlation data for the entire observation. It corrects for the changing optical path delay, and performs the calibration between the ON/OFF measurements.

2.5 Data Reduction

The stored data consists of a series of correlograms, c_j, that correspond to the averaged cross-correlation of the number of photons registered in channel 1 or 2, represented by N_1 and N_2, at time t_i over an accumulation period of T_a,

$$c_j(t_i, k) = \langle N_1(t_i) N_2(t_{i+k}) \rangle_i. \tag{1}$$

The notation $\langle ... \rangle_i$ represents the average with respect to the quantity i. The delay applied between the two channels for the calculation of the correlation is represented by k in units of sampling time. The normalized second-order correlation function is then calculated by dividing Equation (1) by the product of the average numbers of photons per sample counted over the same accumulation period in the two channels

$$g_j^{(2)}(k) = \frac{\langle N_1(t_i) N_2(t_{i+k}) \rangle_i}{\langle N_1(t_i) \rangle_i \langle N_2(t_i) \rangle_i}. \tag{2}$$

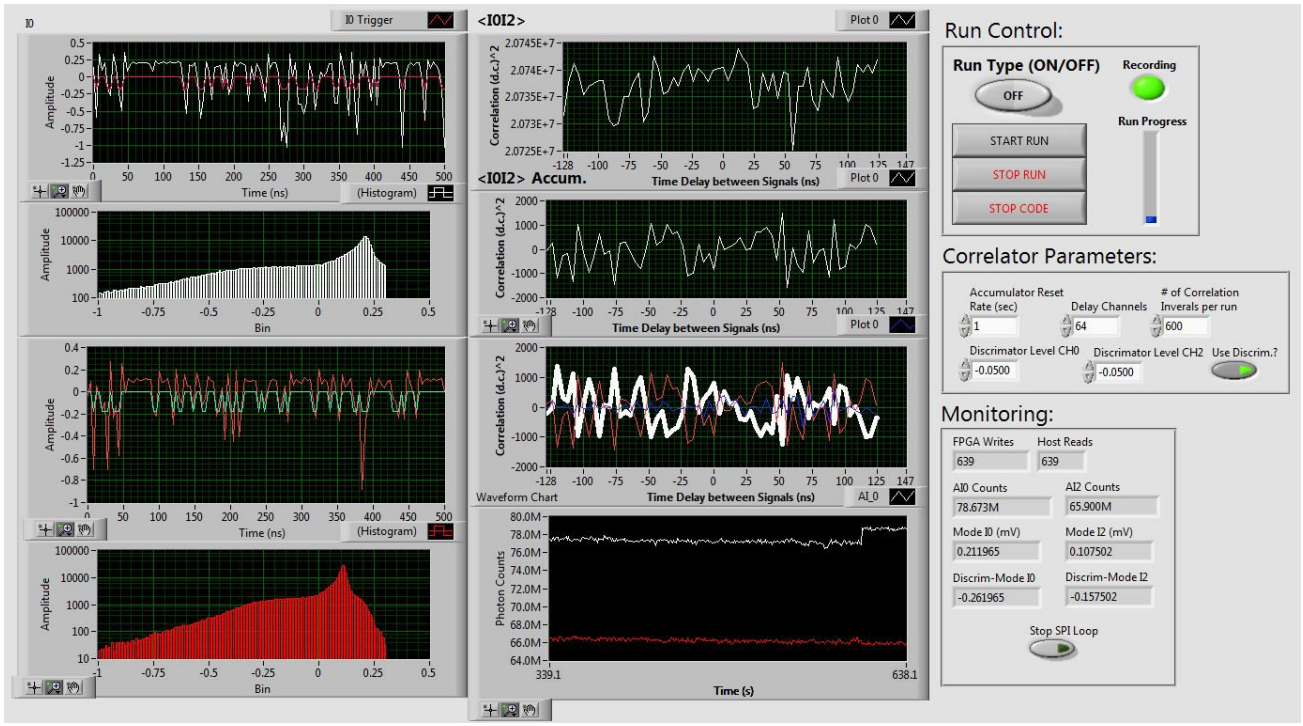

Figure 2: Screen shot of the observing interface for SII measurements at StarBase during an observation of Regulus. On the left side, the first and third panel from the top display the traces of the signal recorded at the ADC input shown for the separate channels (white and red) each overlaid with the photon trigger (pink and aqua blue). The top three middle panels display the correlogram in different configurations. The top shows the correlogram obtained every accumulation period, the middle shows the integrated correlation over the current run, and the third shows the ON, OFF, and ON-OFF correlation. The last panel in the middle section displays the photon counts over the previous 5 minutes of observation. The parameters on the right include the configuration settings for the discriminator level and correlator, and also controls for the run type.

To account for any drift in the level of the signal, each of these correlograms are subtracted by the average value measured across the correlogram excluding the m delay channels that are within one sampling time interval of the optical path delay at the time of observation

$$f_j = g_j^{(2)}(k) - \langle g_j^{(2)}(k) \rangle_{k \neq m}. \tag{3}$$

An averaged ON and OFF measurement is then calculated for each ON or OFF cycle (i.e. $f^{ON} = \langle f_j^{ON} \rangle_j$). For each correlogram, the scatter across all time-delay bins should be randomly distributed arising from the correlation of shot noise in each of the detectors. However, the detection of spurious correlations, attributed to radio frequency interference, sets a limit to the achievable sensitivity. To remove these spurious correlations the averaged OFF correlogram is scaled and subtracted from each ON accumulation by

$$f_j^{\Delta} = f_j^{ON} - b f^{OFF}. \tag{4}$$

A scaling factor b accounts for differences in the amplitude of the spurious correlation between the ON and OFF runs. Here we choose b such that it minimizes the root-mean-square (RMS) value of the residual ON-OFF correlation as measured across all delay channels,

$$b = \frac{\langle f^{ON}(k) f^{OFF}(k) \rangle_{k \neq m}}{\langle f^{OFF}(k) f^{OFF}(k) \rangle_{k \neq m}}. \tag{5}$$

To account for the optical delay, τ_o, each noise subtracted ON correlogram is interpolated, then shifted in time by the value of the optical path delay for the time the measurement was taken (i.e. $f_j^{\Delta} \rightarrow f_j^{\Delta}(t - \tau_o)$). After

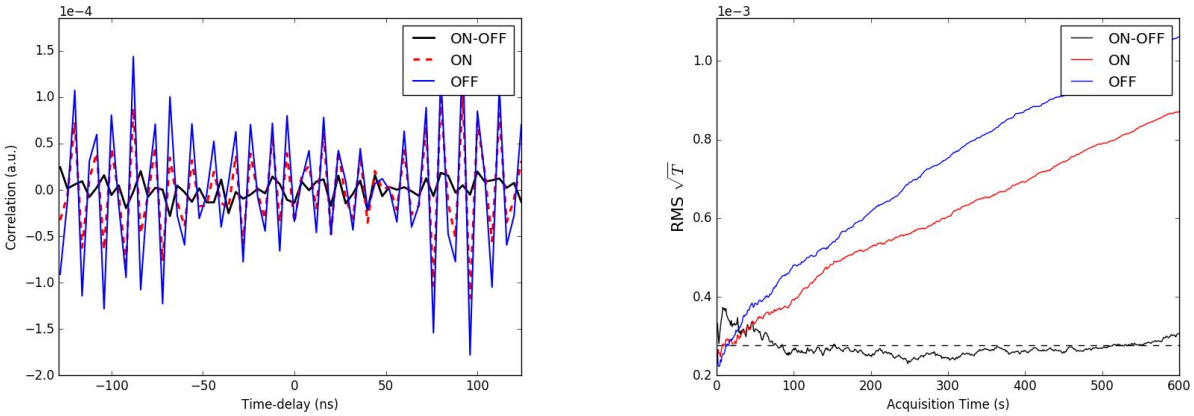

Figure 3: LEFT: The correlation as a function of the time-lag averaged over the length of a single ON/OFF cycle during an observation of η UMa at the StarBase observatory. The plot includes measurements for the ON, OFF, and scaled residual ON-OFF. RIGHT: The RMS value of the correlogram as a function of the integration time for ON, OFF, and the scaled residual ON-OFF measurements. Although the ON and OFF runs are limited by spurious correlations, the sensitivity is improved through the ON-OFF subtraction routine described in section 2.5. The dotted line indicates the expected RMS for the average photon rate observed over the run.

the path delay correction, all of the correlograms are averaged together to produce a final correlogram. The RMS of the integrated ON, OFF, and scaled residual ON-OFF correlogram is calculated to verify that the data reduction is properly performed and is validated by comparison to the expected RMS according to counting statistics. Figure 3 illustrates typical results using the data reduction routine.

The reduction routine described above provides an effective way to obtain initial results in the low SNR regime where the necessary observation time is on the order of several hours. During the observation, the instantaneous projected baseline is changing continuously, and correspondingly, the expected coherence. By averaging the measurements obtained throughout the night, the information over all projected baselines for a single pair of telescopes is effectively reduced into a single baseline. For the case where integration times need to be greater than several hours this seems unavoidable, however, for larger telescopes with greater bandwidth, the integration time can be brought down to minutes, if not less. In this case, the data reduction can be segmented in order to retrieve the information as a function of the (u,v) plane separation.

3. LABORATORY RESULTS

Before carrying out measurements with the StarBase telescopes, the data acquisition modules and correlator were tested in the laboratory in order to validate the capabilities of the hardware and analysis. To simulate star-light, light from the 435.8 nm spectral line of a mercury arc-lamp light source is focused onto a 0.3 mm pinhole. The light from the pinhole travels approximately 3 m before reaching a beamsplitter and then it is detected by separate PMTs. The light-sensitive area of the PMT is covered using a mask with a 5 mm diameter hole cut out. This was chosen in order to be within than the estimated 6 mm spatial coherence length of the source but large enough to maximize the light flux to allow for relatively short integration times. One of the detectors is mounted onto a linear actuator in order to measure the spatial coherence of the source as a function of the detector separation. The signal from the PMTs are then fed into the hardware system, described in section 2.2, to obtain the cross-correlation.

The OFF background correlation measurements can be done in the laboratory either through i.) selecting orthogonal polarization between detectors (as implemented on StarBase and explained earlier) or ii.) by separating the detectors by an amount that is much greater than the expected spatial coherence length. For the measurements presented herein, it was more convenient to use the latter approach since the movement of the linear actuator can be automated together with the data acquisition.

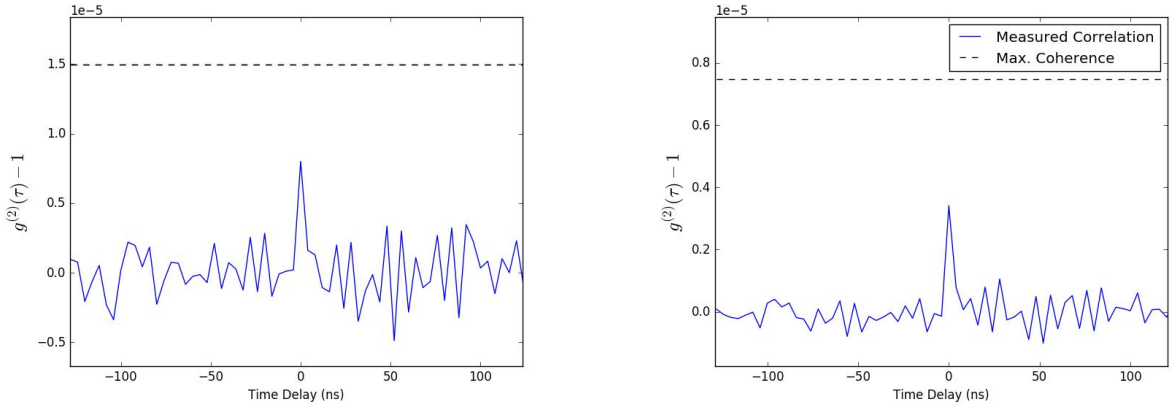

(a) (b)

Figure 4: The above plot shows measurements of the normalized correlation function for a laboratory arc-lamp source in the low (a) and high (b) photon flux regime. The effective spectral line-width of the light source ($\Delta\lambda \approx 5\,\mathrm{nm}$) is similar to the typical filter bandpass width possible when observing starlight, thus making it a good calibration test for performing II measurements. The black dotted line on top displays the maximum of the expected signal under ideal conditions. The calculation of this value is explained in Section 3. In both plots a similar discrepancy between the expected signal and the measurements is apparent. This is largely attributed to internal reflections within the optical setup.

Two laboratory measurements of the $g^2(\tau)$ function for the arc-lamp source are displayed in Figure 4. Our measurement was done in the photon counting regime (left) for relatively low photon flux and the other was done in the linear mode (right) for large photon flux. In the photon counting mode, a linear polarizing filter was inserted before the pinhole in order to reduce the necessary integration time for a given photon rate. ON-OFF correlation measurements were cycled every 5 minutes over a total 'ON' integration period of 7 hours. The averaged count rate for both detectors over the entire observation was measured at 64 MHz. For the observation in the large photon flux regime, ON/OFF cycles were performed every minute over a total integration time of 20 minutes. In both plots the expected value of the coherence signal is plotted. The expected coherence signal can be understood as the ratio between the effective resolution time of the laboratory system and the coherence time of the light. In the case of the photon counting mode measurement, the light is linearly polarized, which doubles the expected signal. A partial coherence factor[2] of 0.474 is included in the calculation of the expected signal which accounts for the finite light-collection area of the detectors. In both of the plots, the measured signal is significantly less than the expectation. We attribute a significant portion of this difference due to internal reflections in the optical system which would reduce the measured signal. Previous tests using psuedo-thermal source light revealed the peak correlation was reduced by up to 50% of the expected value. Additionally, a large systematic uncertainty of the signal remains in the optical bandwidth of the light source.

4. OUTLOOK

The system described in this paper is currently being tested at the StarBase observatory. Two initial targets for observation are the stars Regulus (α Leo) and Alkaid (η UMa). These sources were chosen as the value of the second order spatial coherence function $|\gamma(d)|^2$ for the StarBase baseline is relatively large. This allows for verification of the instrumentation in reasonable observation times. The expected significance of an observation lasting over a time period of T_0 for a source of spectral flux η (ph/s/Hz/m^2) can be written in a first approximation as[21]

$$SNR = \beta_0 A \alpha \eta |\gamma(d)|^2 \sqrt{\frac{\Delta f T_0}{2}}. \tag{6}$$

The expected SNR is linearly dependent on the light-collection area of the telescope A, detector quantum-efficiency α, and on the square root of the electronic bandwidth Δf. To account for polarization resolved

measurements a polarization factor β_0 is included which is equal to 1 in the case of unpolarized light and 2 for linearly polarized light. Equation (6) can then be rewritten in terms of the total observation time needed for a desired SNR:

$$T = \left(\frac{SNR}{\beta_0 A \alpha \eta |\gamma(d)|^2} \right)^2 \frac{2}{\Delta f}. \tag{7}$$

In the case where the data is processed using the ON-OFF reduction routine, the required integration time is then doubled due to the statistical error introduced in the subtraction. Using the observed PMT rates from preliminary observations of Alkaid and Regulus, the expected observation time for a $5\,\sigma$ measurement is on the order of 7 hours of ON observation time.

Here, it is important to note that the StarBase observatory establishes a lower limit to the II capabilities of other IACT observatories. As shown in Equation (7), the total observation time needed for a given star is inversely proportional to the square of the light collection area. Thus, the VERITAS reflectors,[22] with an area approximately 16 times greater than the StarBase telescopes, could observe a similar source at the same significance in 1/256th of the time. This assumes the same source brightness and spatial coherence. By porting the StarBase system onto the VERITAS telescopes, the integration time of 7 hours would be reduced to slightly over 1.5 minutes. Such capabilities allow measurements at multiple projected baselines for a single a pair of telescopes, and potentially even polarization resolved measurements.

Further improvements could be made by taking advantage of the 0.6^o PSF of the VERITAS telescopes[23] to allow for reasonably sized collimating lens. The collimating lens would reduce degradation of the optical bandwidth through the interferometric filter. Additionally, the electronic bandwidth could be improved by using an ADC with faster sampling. In practice, the bandwidth can be improved up to the limit where the sampling time is shorter than the time dispersion of photons in the focal plane or the rise-time of the detector response. For IACT telescopes of the Davies Cotton optical design, this dispersion is generally on the order of a few nanoseconds suggesting a maximum bandwidth up to approximately 1 GHz.

5. SUMMARY

This paper presents the development of a digital SII system prototype and its operation with a pair of telescopes similar in design to IACT observatories. The issues of fast focal ratios can be improved by using interferometric filters where the coating displays a high refractive index. Although the modest optical quality of IACT observatories creates difficulties in filtering the light, this is compensated for by the large light collection area offered. A digital SII acquisition and analysis system is presented using high-speed ADC conversion and FPGA based processing. Laboratory results have demonstrated the capability of the system to perform II measurements comparable to stellar sources over a large range of photon rates. Such tests demonstrate the ability to scale the system over a range of observable stellar magnitudes or telescope sizes. Forthcoming results at StarBase will validate the system for stellar sources. The system can be readily scaled to current observatories. Plans to integrate the system with the VERITAS observatory is intended for Fall 2018. An implementation of the system onto the VERITAS observatory would allow for $5\,\sigma$ measurements of bright sources in observations lasting only a few minutes. Such observations would provide valuable experimental constraints to an SII implementation on the future CTA observatory.

ACKNOWLEDGMENTS

The authors gratefully acknowledge financial support for this work by the University of Utah and through US National Science Foundation grants AST 1806262 and PHY 1510504. NKM acknowledges travel support from the National Instruments Academic Travel Research Grant and the Willard L. Eccles Foundation. The authors of this paper would like personally thank George Sanders and Linda Smith Nelson at the Bonneville SeaBase (http://www.seabase.net/) in Grantsville, Utah.

REFERENCES

[1] Hanbury Brown, R., Davis, J., and Allen, L. R., "The angular diameters of 32 stars," *Monthly Notices of the Royal Astronomical Society* **167**(1), 121 (1974).

[2] Hanbury-Brown, R., [*The Intensity Interferometer. Its applications to astronomy*], Taylor & Francis (1974).

[3] Pilyavsky, G., Mauskopf, P., Smith, N., Schroeder, E., Sinclair, A., van Belle, G. T., Hinkel, N., and Scowen, P., "Single-Photon Intensity Interferometry (SPIIFy): utilizing available telescopes," *Monthly Notices of the Royal Astronomical Society* **467**, 3048–3055 (May 2017).

[4] Guerin, W., Dussaux, A., Fouch, M., Labeyrie, G., Rivet, J.-P., Vernet, D., Vakili, F., and Kaiser, R., "Temporal intensity interferometry: photon bunching in three bright stars," *Monthly Notices of the Royal Astronomical Society* **472**(4), 4126–4132 (2017).

[5] Zampieri, L., Naletto, G., Barbieri, C., Barbieri, M., Verroi, E., Umbriaco, G., Favazza, P., Lessio, L., and Farisato, G., "Intensity interferometry with Aqueye+ and Iqueye in Asiago," in [*Optical and Infrared Interferometry and Imaging V*], *Proc. SPIE* **9907**, 99070N (Aug. 2016).

[6] Tan, P. K., Yeo, G. H., Poh, H. S., Chan, A. H., and Kurtsiefer, C., "Measuring Temporal Photon Bunching in Blackbody Radiation," *The Astrophysical Journal* **789**, L10 (July 2014).

[7] Tan, P. K., Chan, A. H., and Kurtsiefer, C., "Optical intensity interferometry through atmospheric turbulence," *Monthly Notices of the Royal Astronomical Society* **457**, 4291–4295 (Apr. 2016).

[8] Tan, P. K. and Kurtsiefer, C., "Temporal intensity interferometry for characterization of very narrow spectral lines," *Monthly Notices of the Royal Astronomical Society* **469**, 1617–1621 (Aug. 2017).

[9] Trippe, S., Kim, J.-Y., Lee, B., Choi, C., Oh, J., Lee, T., Yoon, S.-C., Im, M., and Park, Y.-S., "Optical Multi-Channel Intensity Interferometry - Or: How to Resolve O-Stars in the Magellanic Clouds," *Journal of Korean Astronomical Society* **47**, 235–253 (Dec. 2014).

[10] Matthews, N., Kieda, D., and LeBohec, S., "Development of a digital astronomical intensity interferometer: laboratory results with thermal light," *Journal of Modern Optics* **0**(0), 1–9 (2017).

[11] LeBohec, S. and Holder, J., "Optical intensity interferometry with atmospheric cerenkov telescope arrays," *The Astrophysical Journal* **649**(1), 399 (2006).

[12] Rou, J., Nuñez, P. D., Kieda, D., and LeBohec, S., "Monte Carlo simulation of stellar intensity interferometry," *Monthly Notices of the Royal Astronomical Society* **430**, 3187–3195 (Apr. 2013).

[13] Acharya, B. et al., "Introducing the cta concept," *Astroparticle Physics* **43**, 3 – 18 (2013). Seeing the High-Energy Universe with the Cherenkov Telescope Array - The Science Explored with the CTA.

[14] Bigongiari, C., "The cherenkov telescope array," *Nuclear and Particle Physics Proceedings* **279-281**, 174 – 181 (2016). Proceedings of the 9th Cosmic Ray International Seminar.

[15] Nunez, P. D., *Towards optical intensity interferometry for high angular resolution stellar astrophysics*, PhD thesis, The University of Utah (2012).

[16] Nuñez, P. D., Holmes, R., Kieda, D., Rou, J., and LeBohec, S., "Imaging submilliarcsecond stellar features with intensity interferometry using air Cherenkov telescope arrays," *Monthly Notices of the Royal Astronomical Society* **424**, 1006–1011 (Aug. 2012).

[17] Dravins, D., LeBohec, S., Jensen, H., and Nuez, P. D., "Optical intensity interferometry with the cherenkov telescope array," *Astroparticle Physics* **43**, 331 – 347 (2013). Seeing the High-Energy Universe with the Cherenkov Telescope Array - The Science Explored with the CTA.

[18] Garstang, R. H., "Night sky brightness at observatories and sites," *Publications of the Astronomical Society of the Pacific* **101**(637), 306 (1989).

[19] LeBohec, S., Adams, B., Bond, I., Bradbury, S., Dravins, D., Jensen, H., Kieda, D. B., Kress, D., Munford, E., Nuñez, P. D., Price, R., Ribak, E., Rose, J., Simpson, H., and Smith, J., "Stellar intensity interferometry: experimental steps toward long-baseline observations," in [*Optical and Infrared Interferometry II*], *Proc. SPIE* **7734**, 77341D (July 2010).

[20] Otte, A. N., "The upgrade of veritas with high efficiency photomultipliers," in [*32nd International Cosmic Ray Conference*], (2011).

[21] Brown, R. H. and Twiss, R. Q., "Interferometry of the intensity fluctuations in light ii. an experimental test of the theory for partially coherent light," *Proceedings of the Royal Society of London A: Mathematical, Physical and Engineering Sciences* **243**(1234), 291–319 (1958).

[22] Holder, J. et al., "Status of the veritas observatory," *AIP Conference Proceedings* **1085**(1), 657–660 (2008).

[23] Holder, J. et al., "The first veritas telescope," *Astroparticle Physics* **25**(6), 391 – 401 (2006).